INSTRUMENTED WIND TUNNEL FOR SPRAY DRIFT STUDIES

Muhammad Farooq, Dvoralai Wulfsohn and Ron J. Ford

ABSTRACT

An instrumented wind tunnel was developed to study the drift from sprayer nozzles under controlled and repeatable environmental and spraying conditions. The wind tunnel has a 1 m^2 cross section and a 4 meter long testing section. Wind speed and wind direction, nozzle operating pressure, flow rate and height can be controlled and measured while relative humidity and temperature is recorded. An image of the spray sheet frozen against a matt black background is obtained on Black & White film using a series of electronic flashes and a 35 mm SLR camera set to an aperture of 5.6.

A flat fan nozzle was tested at wind speeds of 0, 1.4, 2.8 and 4.2 m/s and operating pressures of 205, 275 and 345 kPa with 3 replicates. Analysis of the images of the spray sheet revealed that the system responded in a meaningful way to changes in environmental and spray parameters. It was confirmed that the wind tunnel was able to produce repeatable conditions.

INTRODUCTION AND BACKGROUND

There is still a need to minimize spray drift from agricultural sprayers. New sprayer systems, designed to fulfill this need, frequently arrive on the market, with unverified claims about reduction in drift (Wolf 1992). Ford (1975) points out that these claims are generally over-optimistic, based more on a belief in what 'ought' to work rather than on sound testing and evaluation. SACAM (1994) recommended that commercial crop sprayers be assessed for their potential loss of agricultural chemicals through large drop drip-off and drift losses.

In field and laboratory studies, the sampling layouts arranged on the downwind side of the spray swath, mostly spread over wide areas (Nordby and Skuterud 1975; Fox et al. 1993; Picot et al. 1993). On the other hand, results of field studies are generally not consistent (Salyani and Cromwell 1992; Bouse et al. 1992). The range of samplers used to collect the spray drift in field and laboratory studies, as cylindrical collectors (Miller and Hadfield 1989), paper (Reichard et al. 1992), mylar sheets (Bouse et al. 1994), plant leaves (Howard 1993) and others (Miller, 1993) are quite inconsistent in providing information on the drift. Deposits from collectors at the same location have been reported to differ by 100 % (Fox et al. 1993a)

The study of drift in a wind tunnel has the advantage of controlling and repeating the spraying and atmospheric conditions. Flow visualization, a technique of making invisible flows visible, combined with wind tunnel and image processing provides an opportunity to study spray droplets under controlled conditions after they are just released from the atomizers.

The objective of this study was the development of an instrumented wind tunnel for estimation of spray drift under varying environmental and sprayer operating conditions. The scope of the instrumented wind tunnel was limited to provide the capabilities as: (1)

visualization of wind flow pattern inside the wind tunnel; (2) measurement of environmental factors; (3) control and measurement of spraying parameters; and (4) acquisition of a digital image of the spray pattern for analysis using image processing.

WIND TUNNEL DESIGN

An instrumented wind tunnel was developed with the following features: (a) Provision for altering the spraying conditions, i.e., wind speed, wind direction in reference to orientation of nozzle, height above the crop, operating pressure and flow rate; (b) Provision to monitor and record environmental variations, i.e., wind speed profile, temperature and relative humidity; (c) Capability to acquire a frozen image of the spray sheet; and (d) Provision for using a variety of spray nozzle types and sizes.

The designed wind tunnel consists of a basic tunnel structure, a suction fan, flow straighteners, spraying and spray control system, flow visualization unit, image acquisition unit and instrumentation (Figure 1). The entire set up is 6.5 m long, 1 m wide, 2 m high, movable and costed less than $ 10,000.

The wind tunnel has 4 m long test section with see through front wall used to take the image of spray and air flow patterns. The cross section of the tunnel increases from 0.91 m x 0.91 m at the entrance to 1 m xl m at the exit with a slope of 0.5“ which reduces the friction of the walls to air, minimize the effect of boundary layer and maintain uniform wind speed through out the section (Pope and Harper 1966). The tunnel contains entrance and exit ducts shaped to smooth air flow at both ends of the tunnel. The transition duct, between the main tunnel and exit duct helps to get a diversion angle of 6” to air flow, within the 5-7” recommended for smooth transition from a rectangular to a circular cross section (Pope et al. 1966). Two acrylic windows at the top of the tunnel are used to illuminate the spray pattern. Two flow straighteners one each at inlet and exit control the air flow pattern inside the test section. The propeller type suction fan has a maximum discharge of 9.44 m^3/s which accounts for wind speed of 10 m/s in the wind tunnel. The fan speed controlled through an AC inverter allows average wind speeds inside the tunnel from 0.8 to 10 m/s.

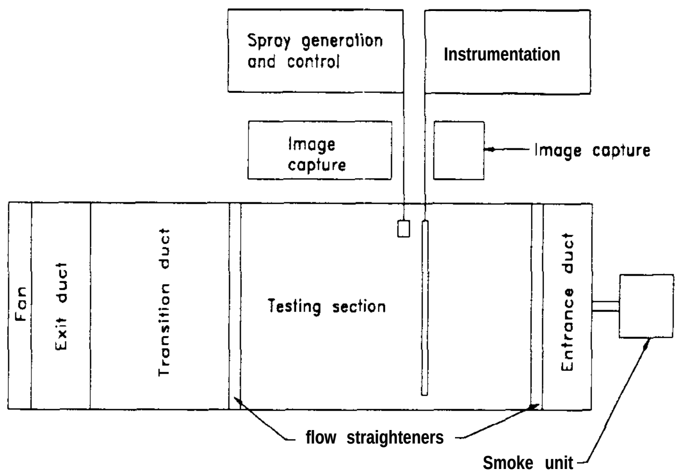

Figure 1: Block diagram of instrumented wind tunnel

The spraying and spray control unit is used to develope spray and, to control and measure spray variables, i.e., operating pressure and flow rate. The nozzle fixed to a brass bushing is inserted from top of the tunnel, can be moved up or down or can be rotated. The brass bushing can accommodate commonly used nozzle bodies. A pointer on top of the tunnel, indicates height of the nozzle from the floor of the wind tunnel. The visualization unit makes the air flow inside the tunnel visible which is used to confirm the laminarity of the air flow along the length of the tunnel. A gray smoke is generated by exploding a smoke bomb into a heavy duty plastic barrel. The smoke is injected into the tunnel from four equally spaced pipes along the vertical axis through the flow straightener at the entrance. Both air and smoke being at atmospheric pressure and subjected to same suction, maintain same speed in the tunnel. The rate of smoke injection and the density of smoke produced, is controlled with a valve.

After a series of trials on light sources & their position, film speed and camera setting, four units of 100 watt Britek master/slave flash bulbs having a flash duration of 1/850 second and 35 mm SLR camera with B&W, IS0 400 film were selected for image acquisition system. The flash bulbs are installed on top of the wind tunnel and have provision for multi-directional movement to adjust the light intensity and area covered inside the nozzle. The two flash units close to the nozzle are tilted towards the nozzle. The black cards on both sides of the bulbs restrict the light away from background and the plexiglass to avoid reflections which reduces spray/background contrast. The inner of top, bottom and back panels of the wind tunnel is painted flat black to eliminate unwanted reflections. A black cloth between tunnel and camera eliminate reflection on the image from behind the camera.The flash units are connected to the camera by synchronization cables. The shutter speed of the camera is set at 1/60 S but due to short duration of the flash illumination, the image is effectively frozen on the film.

A grid of 24 resistance type sensors is installed to measure wind flow pattern across the wind tunnel or to check the uniformity of the flow. Three sample sensors were calibrated in a bench-type wind tunnel for wind speeds of 0.15-7.5 m/s. Regression analysis resulted in the following equation with coefficient of determination (R^2)= 0.999.

$$\ln V_w = 7.056 - 0.073T + 0.0001\,16T^2 \quad (1)$$

where:

S = Wind speed (m/s)
T = Temperature (“C).

The calibration has an average error of ± 3.32%. The direction of the sensors relative to the wind altered the wind speed measurement up to 20 percent. In higher relative humidity (RH) conditions, sensors give higher wind speeds while in higher temperatures gives lower speeds. Three-point calibration of all the sensors was performed using the same type of model to eliminate any variation due to construction errors. The sensor outputs are recorded by datalogger connected to a 80286-based computer. A Basic program manipulates the emf voltages from sensors to get wind speed in m/s using regression equations developed for each sensor. The program updates the wind speeds after every 4 seconds on the screen and writes to the diskette. A humidity sensor records the relative humidity near the tunnel entrance while a thermocouple records temperature inside the tunnel which are also recorded by the datalogger.

TESTING OF WIND TUNNEL

Tests were conducted to verify (1) that the air flow throughout the cross section of the wind tunnel is uniform and not turbulent, and (2) that the set up alters spray pattern with changes in testing conditions and is capable of providing information for quantification of drift. In both tests, images of flow were recorded using image acquisition. For wind flow pattern, the camera was placed 2.7 m away from the tunnel, and an image captured of the entire length of the testing section. For the spray pattern, the camera was placed 1.0 m away from the wind tunnel to cover area from nozzle to bottom of the wind tunnel, extending 0.75 m from the nozzle to downwind. All the images were taken in complete darkness and the spray lit by the light of the flash bulbs.

Wind flow pattern experiment

For wind flow pattern visualization, smoke flow in the wind tunnel was photographed at wind speed settings of 1.4, 2.8, 4.2, 5.6, 7.0, and 8.4 m/s. Wind speed was also measured with the velocity sensor grid. The relative humidity and temperature inside the tunnel ranged from 55.4 to 58.5% and 20.8" to 21.4 °C, respectively, during these tests.

Results and discussion

Figure 2 is an image of smoke flow inside the wind tunnel at wind speed of 5.6 m/s. This, and other images, indicated laminar flow from three lower outlets while the flow from the upper outlet rises upward at the last half of the testing section. This may be the effect of nozzle just protruding into the top surface of the tunnel. The turbulent eddies were more evident at the speeds of 1.4 and 2.8 m/s than at other speeds. These images may have been taken sooner after release of the smoke compared to the times in other speeds. There is also glare on top of some images due to reflection of light from the plexiglass on top which exaggerates the turbulent eddies. The triangular dead zone in the upper left side of the image is because of the the lights coming from both sides of the nozzle. We calculated Re for the tunnel cross section in the range of 10' but the turbulence is suppressed by the two flow straighteners.

Figure 2: Image of smoke flow in the testing section at wind speed of 5.6 m/s.

The wind speeds measured with the velocity sensors had some spatial variation but were not significantly different at 95% level of significance. The mean, maximum, and minimum wind speeds from all the sensors at different set speeds with standard deviation and coefficient of variation are presented in Table I. To eliminate the effect of relative humidity and air temperature, all wind speeds were adjusted by the same percent as the difference of set speed and the average speed from all sensors. As the direction of the sensor changes the measurement up to 20% of the reading, this may have caused variation among the measurements, suggesting that some form of rigid holding for the sensors is needed.

Table 1: Wind speeds measured by velocity sensors at the different set speeds

Parameter	Set wind speed (m/s)					
	1.4	2.8	4.2	5.6	7.0	8.4
Mean	1.42	2.79	4.25	5.88	7.14	8.48
Maximum	1.95	4.04	5.17	7.40	8.97	10.19
Minimum	1.04	1.96	2.86	3.88	4.58	5.52
Standard deviation	0.22	0.46	0.54	0.79	1.03	1.11
Coefficient of variation	0.16	0.17	0.13	0.13	0.14	0.13
Probability	0.00	0.00	0.00	0.00	0.00	0.00

Spray pattern experiment

<u>Model</u>

We assumed that spatial distribution of particles in a spray sheet is related to particle size. We also assumed that small particles in the spray would reach their terminal velocity before exiting the area in the image and that same sized particles in the spray sheet would be following the same pathlines. We therefore call such pathlines "iso-sized" pathlines. Straight iso-sized pathlines would indicate that particles forming these lines are at terminal velocity and the vertical velocity of the particles is not decreasing.

As defined in Figure 3, θ_o is the angle that the spray sheet makes with the horizontal under no wind. The angle increases to θ_d (deflection angle) because of wind in the given direction. The included angle of the spray sheet (θ_i) changes with pressure change (Teejet 1993) but may not change with wind speed within the range of wind speeds allowed for spraying. The angle θ_l is the slope of the iso-sized pathlines on the image. With increase in wind speed, the slope of these lines

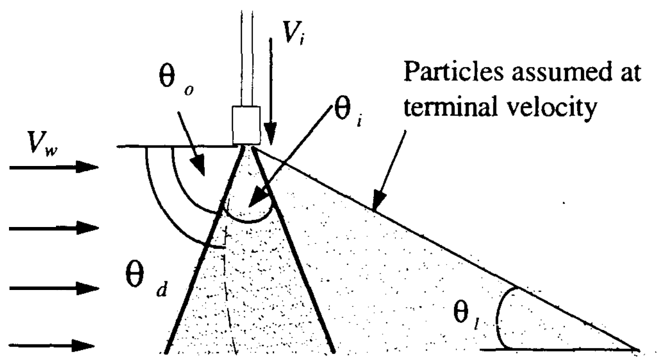

Figure 3: Angles and velocities in spray wind interaction

(θ_t) decreases. The angles θ_o, θ_d and θ_t can be measured from the image using drawing tools available with most image analysis programs. The average wind velocity (V_w) was calculated for each test. The initial spray velocity (Vi), i.e., the velocity of the particles as they exit from the nozzle, depends upon liquid flow rate through the nozzle.

We assumed that water droplets at terminal velocity move at the same speed as the wind in the horizontal direction. Knowing V_w and θ_t for droplets at terminal velocity (downwind of the nozzle), terminal velocity (V_t) of the particles can be determined from:

$$V_t = V_w \times \tan\theta_t \qquad (2)$$

Then the size of the droplets can then be estimated using the following equation when the particle Re is up to 2 (Mohsenin 1986) which in this study ranged from 0.2 to 1.4.

$$d_p = 10^6 \sqrt{\frac{18\eta V_t}{g(\rho_p - \rho_f)}} \qquad (3)$$

where:

d_p = Particle diameter (μm)

ρ_p = Density of droplet, i.e., water = 1000 $kg.m^{-3}$

ρ_f = Density of the fluid (i.e., air) = 1.206 $kg.m^{-3}$

η = Viscosity of the air = 1.78 x 10^{-5} Pa.s

g = Acceleration due to gravity = 9.8 1 $m.s^{-2}$

Exeeriment

A flat fan nozzle, was tested under various spray operating pressures and wind speeds. The experiment was two factor factorial with 4 wind speeds (S 1 = 0 m/s; S2 = 1.4 m/s; S3 = 2.8 m/s; and S4 = 4.2 m/s), 3 operating pressures, (P1 = 205 kPa; P2 = 275 kPa; and P3 = 345 kPa) and 3 replicates (R) for a total of 36 tests. The experimental design was completely randomized with the tests randomized over time. For each test, operating pressure was set and recorded after it was stabilized. The wind speed was set by adjusting the input frequency to the fan. Liquid flow rate for each test was recorded using the flow meter. Average wind speed, tunnel temperature and relative humidity were recorded by the datalogger.

The prints of the images were digitized using CCTV camera and the image analysis program NIH Image 1.55. Using drawing tools available with this program, iso-sized lines were drawn at three locations on the images as in Figure 4. Location 1 was selected as the top edge of the image on the downwind side while locations 2 and 3 were selected where the straight lines were visible. The slopes of these lines were determined by the program. From the slopes of these lines, the terminal velocity of the water droplets was determined using equation 2, while the size of the particles was determined using equation 3. The data obtained for slope, terminal velocity and particle size were analyzed by analysis of variance technique using SPSS to determine whether the effect of wind speed (V_w), pressure (P) and replicate (R) on the slope

(8,), terminal velocity (V,), and particle diameter (d_p) was significant and to test the expected relationship of V_w with θ_l and θ_d and relation of P with θ_i and 8,.

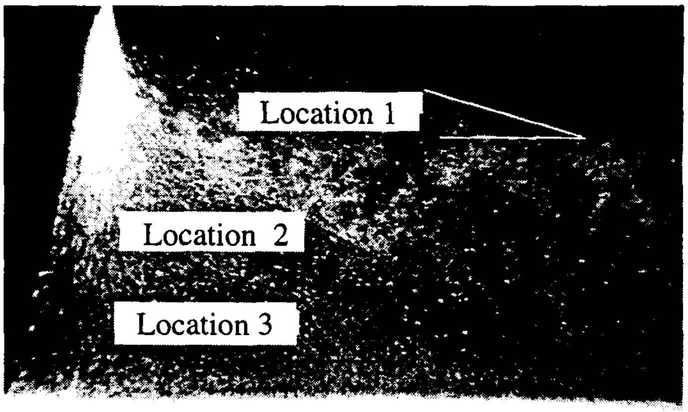

Figure 4: Establishment of iso-sized pathlines on an image

Results and discussion

A t-test showed that the θ_l, V_t and d_p obtained for each location from all images were not significantly different. The comparisons of θ_i and θ_d from each image, separately, using a t-test showed that both of the angles on all images were not significantly different (P < 0.001)

The analysis of variance for data at location 1 showed that V_w, P and R did not significantly affect d_p and V,. The V_w significantly affected θ_l while P and R did not significantly affect it. A similar trend of 8, with *V,, was* expected. As the d_p *in* the location 1 was not significantly different, in spite of the significantly different Cl,, this indicated that the spray responded in a meaningful way to variations in these parameters. It also indicates that the response was captured by the images and was traceable by the image analysis.

The d_p at location 2 was not significantly affected by R and P but by V_w (P=0.007). The effect of R, P and V_w on V_t showed the similar trend as for d_p at the location 2. The effect of V_w on θ_l was highly significant while the effect of R and P was insignificant. The d_p at location 3 was significantly affected by P and V_w while it was not significantly affected by the R. The d_p increased with increased V_w which was not expected. It increased with the increase of P from 205 to 275 kPa but slightly decreased with increase in P from 275 to 345 kPa. This trend was also not expected, however it may be attributed to bias in manually selecting a line at location 3. The V_t followed the same trend as did the d_p. The effect of V_w and P on 8, was highly significant while the effect of R was insignificant. The θ_l increased with increase of P from 205 to 275 kPa but slightly reduced with increase in P from 275 to 345 kPa.

The above results indicate that the location of iso-sized lines other than top edge on downwind side is not appropriate for comparison unless the area of interest is marked on the image before its capturing. In other words, the analysis used is helpful only for estimating the drift potential of the particle on the downwind upper edge of the image. There is need to develop a program to estimate the drift potential of the particles on the rest of the image. There is also need to compare the drift data from the tunnel with other techniques and to calibrate the system to find relationship with intensity of the image and number of particles. As the effect of P on θ_l, *V,* and d_p was insignificant, these parameters were averaged over P for each V_w. These averages at locations 1, 2 and 3 are given in Table 2.

Table II: Average particle size, terminal velocity and slope for three speeds (averaged over pressure) at three locations.

Parameter	Wind Speeds (m/s)		
	1.4	2.8	4.2
Location 1			
Slope (degrees)	22.5	13.2	8.3
Terminal velocity (m/s)	0.58	0.66	0.61
Particle size (μm)	137	146	141
Location 2			
Slope (degrees)	33.9	21.4	17.3
Terminal velocity (m/s)	0.94	1.10	1.30
Particle size (μm)	174	188	205
Location 3			
Slope (degrees)	45.5	31.3	24.8
Terminal velocity (m/s)	1.44	1.70	1.93
Particle size (μm)	216	235	251

The average θ_i for V_w of 0, 1.4, 2.8 and 4.2 m/s was 28.7, 26.9, 26.8, and 27.7 degrees, respectively. The average θ_i for P of 205, 275 and 345 kPa was 24.7, 27.2 and 30.7 degrees, respectively. The effect of P on θ_i was highly significant (P=0.001) while the effect of V_w was insignificant (P=0.631) which was expected for these parameters. The angle increased with increase in P. This result again confirms that the images captured the information which was traceable by the image analysis. The θ_d showed an insignificant relationship with V_w (P = 0.287) and significant relationship with pressure (P = 0.006). The difference of θ_d and θ_0 has significant relationship with V_w (P = 0.024) and pressure (P = 0.025).

The results have indicated that the effect of replicate on all the test parameters, i.e., d_p, V_t, θ_i, θ_d and θ_0 was not significant. Thus the wind tunnel can be used to conduct repeatable experiments.

CONCLUSIONS

The results of the testing of the instrumented wind tunnel have led to the following conclusions.

1 The flow inside the test section of the wind tunnel is essentially laminar in the lower 3/4th of the tunnel cross section. This is the portion of the cross-section which is mainly used for the study of nozzles. Although there is variation in measurements of wind speeds among the sensors, the spatial variation across the cross-section is insignificant and random. The presence of the nozzle itself causes some downstream turbulence.

2. The system responds to changes in environmental and spray parameters such as wind speed and operating pressure.

3. The wind tunnel provides similar results for repeated tests.

4. The image acquisition successfully captures the information about spray sheet and spray drift and it was possible to identify and trace relevant information from the image.

RECOMMENDATIONS

1. The flow along the tunnel cross-section does not simulate the wind speed pattern over the crop canopy as a uniform sized grid was used for the flow straighteners. It would be useful to further study the role of flow straighteners, i.e., variable resistance flow straighteners or the use of baffles to simulate wind velocity profile over a crop canopy.

2. It is recommended that an alternate rigid holding for the velocity sensors inside the tunnel be designed and implemented.

3. There is yet a need to develop an image analysis program that automates the analysis process and transforms information in the image about number of particles, particle velocities and size of particles to potential drift of particles.

4. The system should be calibrate for particle sizes using mono-sized droplet generators.

REFERENCES

Bouse , L.F., J.B. Carlton, I.W. Kirk, and T.J. Hirsch, Jr. 1994. Nozzle selection for optimizing deposition and minimizing spray drift for the AT-502 air tractor. Trans. ASAE. 37: 1725173 1.

Bouse, L.F., S.G. Whisenant, and J. B.Carlton. 1992. Aerial spray deposition on mesquite. Trans. ASAE. 35:5 l-59.

Ford, R.J. 1975. A method for the comparative evaluation of drift abatement techniques for ground sprayers. Can. Agric. Eng. 18:21-22.

Fox, R.D., F.R. Hall, D.L. Richa
rd, R.D. Brazee, and H.R. Krueger. 1993. Pesticide tracers for measuring orchard spray drift. Trans. ASAE. 36:501-505.

Fox, R.D., D.L. Richard, R.D. Brazee, C.R. Krause and F.R. Hall. 1993a. Downwind residues from spraying a semi-dwarf apple orchard. Trans. ASAE. 36:333-340.

Howard, K.D. 1993. Use of mechanical shields for increased deposition. ASAE Paper No. 93-1545, ASAE, St Joseph MI 49085.

Miller, P.C.H. 1993. Spray Drift and Its Measurement. In: G.A. Matthews and E.C. Hislop (Ed.), Application Technology for Crop Protection, CAB International, Wallingford, UK., 101 pp.

Miller, P.C.H., and D.J. Hadfield. 1989. A simulation model of the spray drift from hydraulic nozzles. J. Agric. Engng. Res. 42:135-147.

Mohsenin, N.N. 1986. Physical properties of plant and animal materials- Structure, physical characteristics and mechanical properties. Gordon and Breach Science publishers.

Nordby, A., and R. Skuterud. 1975. The effect of boom height, working pressure and wind speed on spray drift. Weeds Research. 14:385-395.

Picot, J.J.C., D.D. Kristmanson, R.E. Mickle, R.B.B. Dickison, C.M. Riley, and C.J. Wiesner. 1993. Measurement of folial and ground deposits in forestry aerial spraying. Trans. ASAE. 36:1013-1024.

Pope, A., and J.J. Harper. 1966. Low speed wind tunnel testing. John Wiley and Sons, Inc., New York.

Reichard, D.L., H. Dhu, R.D. Fox, and R.D. Brazee. 1992. Computer simulation of variables that influence spray drift. Trans. ASAE. 35:1401-1407.

SACAM. 1994. Saskatchewan Advisory Committee on Agricultural Meteorology, Recommendation 3: Study on Commercial Crop Sprayers. Saskatchewan Advisory Council for Agriculture, Recommendations Report, April 1994,9 pp.

Salyani, M., and R.P. Cromwell. 1992. Spray drift from ground and aerial applications. Trans. ASAE. 35:1113-1120.

Teejet. 1993. Agricultural spray products. Catalog 43A. Spraying Systems Co. Wheaton. IL.

Wolf, T.M. 1992. Novel approaches to spray delivery. Proceedings of APPLI-TECH '92 conference: Agricultural Chemical Application Technology in the '90s, June 17-19 1992, Regina, SK.